Prediction of soil textural constituents using reflected spectra in eastern Mazandaran Province

Nastaran Shiati[1], Seyed Mostafa Emadi[2], Majid Danesh[3†] and Mohammad Ali Bahmanyar[4]

[1] MSc Student, [2] Associate Professor [3] Assistant Professor and [4] Professor, Department of Soil Science, Sari Agricultural Sciences and Natural Resources University, Sari, Iran

†*Corresponding Author Email: m.danesh@sanru.ac.ir*

ABSTRACT

Textural components of soil play an essential role in erodibility and should be considered in many projects of conservation and environmental modeling processes. Traditional methods of determining soil texture are usually laborious, expensive and time consuming along with destructive effects on the environment. Meanwhile, spectroscopic technology using the spectral features and signatures from the whole reflected spectra of soil surface promises a competent method to study soil constituents. To investigate this issue, 113 points were selected and sampled randomly from 0-15 cm of soil surface in eastern parts of Mazandaran Province, Iran. Samples were haphazardly divided into 91 for model building and 22 for final verification and accuracy assessment processes. Applying the enhanced PLS-algorithm plus the FLOOCV approach along with spectral transformations and pre-processing, the modeling of each textural components were accomplished. Spectrally, sand and clay fractions were modeled with high accuracy as: $R^2_c = 0.89$, $RMSE_c = 7.42$, $SE_c = 7.46$ for sand and $R^2_c = 0.82$, $RMSE_c = 6.88$, $SE_c = 6.92$ for the clay content. Whereas, the silt predictive model was slightly weaker than the other constituents. The most effective spectral ranges involved in the modeling process, were also detected and recognized based on beta & spectral weight analyses and Marten's uncertainty test. Additionally, the most influential spectroscopic ranges included were the visible, NIR and SWIR regions with the specified wavelengths. In general, the efficacy of spectroscopic technology in soil texture studies has been proven by this research. Using the computed spectral models, we are able to study the soil textural components at large scales faster, safer, timelier and also cheaper. That is absolutely true and applicable using the regionalized remotely sensed data but requires further investigation in different geographical regions.

Keywords: FLOOCV approach, PLS-algorithm, soil conservation, Spectroscopy, textural constituents.

List of abbreviations

ANOVA	Analysis of variance	PLS/PLSR	Partial Least Squares/Partial Least Squares Regression algorithm
ASD-FieldSpec III	Analytical Spectral Device FieldSpec3	PMs	Parent Material(s)
ATR	Attenuated Total Reflectance spectra	PSD	Particle Size Distribution (soil constituents)
BRDF	Bidirectional Reflectance Distribution Function(s)	$R_{c/p/cv}$	Correlation coefficient for calibration/prediction/cross-validation subsets
CHRIS-PROBA sensor	The Compact High-Resolution Imaging Spectrometer (CHRIS) onboard the Project for On-Board Autonomy (PROBA) satellite sensor	$R^2_{c/p/cv}$	Coefficient of determination for calibration/prediction/cross-validation subsets
CV	Coefficient of variation (%)	$RMSE_{c/p/cv}$	Root mean square error for calibration/prediction/cross-validation subsets
CR method	Continuum Removal method	$RPD_{c/p}$	Ratio of Performance to Deviation or Residual Prediction Deviation calibration/prediction subsets

CV(s)/FCV	Cross Validation(s)/ Full-Cross Validation algorithm		RPIQ c/p	Ratio of Performance to InterQuartile distance calibration/prediction subsets
D-transformation	Derivative transformation algorithm		SE c/p	Standard Error for calibration/prediction subsets
GPS	Global Positioning System		SG-Filter/Algorithm	Savitzky-Golay Filtering Algorithm
IFt	Influence test		SNR	Signal-to-Noise Ratio
LDRS	Lab Diffuse Reflectance Spectroscopy		SMR	Soil Moisture Regime
FOV	Field of View		SOM	Soil Organic Matter
FLOOCV/LOOCV	Full-Leave-One-Out-Cross-Validation/Leave-One-Out-Cross-Validation		SSRC(s)	Soil Spectral Reflectance Curve(s)
KS	Kolmogorov-Smirnov test		STR	Soil Temperature Regime
LV(s)/LF(s)	Latent Vector(s)/Latent Factor(s)		VNIR-MIR	Visible-Near Infrared-Middle Infrared
MIVIS sensor	Multispectral Infrared and Visible Imaging Spectrometer sensor		VNIR-DRS/VNIRS	Visible-Near Infrared-Diffuse Reflectance Spectroscopy/Visible-Near Infrared Spectroscopy Technology
mm/nm	Millimeter/Nanometer		VOI	Variable of Interest
MLR	Multiple Linear Regression		UV-Vis-NIR-SWIR	Ultraviolet-Visible-Near Infrared-Short Wave Infrared hyperspectral ranges
PC(s)R/PCA	Principal Component (s) Regression/Principal Component Analysis			

1. Introduction

Soil textural fractions play essential and fundamental roles in a wide range of soil properties and processes. In other words, soil textural components are interconnected with other soil characteristics and strongly influence them. For instance, textural components directly affect the formation of aggregates and soil structural attributes. Hence, it should be taken into accounts in many plans and projects of soil erosional management, conservation, and environmental modeling. Also it is very important in decision making polices for soil productivity, environmental support and sustained management of agriculture (Qi *et al.*, 2018). Particularly soil textural components play an influential and essential role in soil conservation especially in areas prone to all types of soil erosion (Ostovari *et al.*, 2018). However, determination of soil forming components using the conventional laboratory methods is normally pricey, tiresome, time-consuming and destructive to the environment, particularly at large scales (Bahrami *et al.*, 2022; Peng *et al.*, 2020). Hence, an agile, comfortable and high-accurate approach to study this soil characteristic is urgently required. The high-tech approach of working with reflected spectra such as spectroscopy is usually quick, inexpensive, simply repeatable, minimal need to sample pretreatment, and without environmental disturbance (Peng *et al.*, 2020; Zhao *et al.*, 2020;). Then, this state-of-the-art approach has increasingly become popular as is nondestructive, straightforward, timely and cost-effective (Ji *et al.*, 2016; Xu *et al.*, 2018ab). This technology can be a supplement or substitute for conventional soil characterization approaches as well. The spectral reflectance curve is a fingerprint for each soil which is calculated and plotted using the spectroscopic device (Danesh *et al.*, 2022). Accordingly, spectral features and signatures contained in the reflected spectra can be related to the soil characteristics such as soil particle composition (Ostovari *et al.*, 2018; Padarian *et al.*, 2019; Xu *et al.*, 2018ab). The techniques of spectroscopy are likewise well-structured to be used as

handheld or portable in a field. As a rule, spectroscopy is the exploration of the interaction of soil materials with incident light in a specific spectral range. This technology takes advantage of combinations and overtones of fundamental vibrations from molecular spectral absorption in the region of MIR (Mura *et al.*, 2019). Combinations and overtones spectrally occur in NIR-SWIR region which is related to the vibrational modes of structural groups and bonds such as -CH, -OH and -NH (Mura *et al.*, 2019). Mathematically, various spectral models have been used to make connections between soil properties and spectral data. They all intend to explore more precise information about the soil forming components (Hong *et al.*, 2019). Among them, the PLS algorithm is common and widely used which has also strong multi-component analytical approach, because it can cope with the multi-collinearity errors and handle highly dimensional spectral data (Guo *et al.*, 2019; Peng *et al.*, 2020). The ability of predicting soil properties such as SOM, clay minerals, moisture, etc. using spectroscopy technology has been reported in some studies (Danesh and Bahrami, 2022; Danesh *et al.*, 2022; Xia *et al.*, 2015; Xu *et al.*, 2018). It is of great importance that some soil characteristics can be investigated simultaneously applying a single scanning by spectroscopic device. Xu *et al.*, (2018 ab) assessed important properties related to the Soil Taxonomy in China using vis-NIR spectroscopic technology. Altogether, this spectral reflectance sensing method is seen as an influential substitute to prevalent lab analyses while it can examine several properties synchronously (Ji *et al.*, 2014; Viscarra Rossel and Webster, 2012; Xu *et al.*, 2018). Some major soil properties have been modeled using vis-NIR technology integrated with the PLS algorithm and the performance was evaluated as satisfactory (Peng *et al.*, 2020; Pudełko and Chodak, 2020). However, recently, further investigation on the mentioned approach has been the focus of the studies. Tumsavas *et al.*, (2018) examined the efficiency of vis-NIR technology for assessment of soil texture components in Turkey. The regression coefficient (R^2) and RPD index for modeling of soil fractions were satisfactory and relatively high. Peng *et al.*, (2020) compared the methods of predicting soil properties using spectroscopy and resulted the good indices for spectral models for soil texture in China. Additionally, Danesh *et al.* (2022) and Bahrami *et al.* (2022) studied the capability of the vibrational reflectance spectroscopy to detect spectral signatures and behaviors of texture components in Iran with acceptable model parameters. Regarding the prediction of soil textural components, it has become a major trend to find quick, efficacious and uncomplicated methods. The present study intends to examine the applicability of spectroscopic technology in characterization of soil texture in eastern parts of Mazandaran, Iran. Hence, the objectives were: (1) studying the applicability of spectroscopic technology in

determining soil textural fractions, and (2) assessing the accuracy of analytical chemometric approach using the reflected spectra.

2. Materials and Methods
2.1. The study area

Totally, 113 compound samples were collected from soil surface of 0-15 cm in eastern parts of Mazandaran Province, Iran. The dominant land uses were as forest (natural and manmade), cultivated and agricultural land, orchard and urban, the places of which were between Qa'em-Shahr (36° 28' 6.24" N, 52° 51' 48.24" E) to Beh-Shahr (36° 41' 43.08" N, 53° 32' 11.4" E) with an approximate area of 5788 km^2 and altitude -27 m to +32 m above-sea-level. The region has respectively mean annual temperature and precipitation of 15 °C and 789.2 mm, with predominantly the Xeric and Thermic conditions, referred by STRs and SMRs (Emadi *et al.*, 2020). Soil samples were gathered randomly. The distribution and location of the sample points are shown in Fig. 1.

2.2. Soil lab

In the soil lab, the air-dried samples were crushed and the clods were powdered, then passed through a 2 mm sieve. The textural components were analyzed and determined using the hydrometric method (Camargo *et al.*, 2009). The textural classes of soil samples based on the soil texture triangle are shown in Fig. 2.

2.3. Spectral lab

Spectroscopic operation was fulfilled in the standard dark room (no stray light) using an ASD-FieldSpec III. The absolute reflectance of samples recorded in the range of 350-2500 nm and 1 nm spectral resolution which resulted in 2151 spectral data-points per sample. About 10 g of the dried samples used for spectral analyses. Soil reflectance spectra were scanned via fiber-optic cable with FOV of 25° (no fore-optic). The normalization of the spectra was performed using the white reference panel of Spectralon. Generally, a standard arrangement of the spectral lab was used for all assays with the distance about 10 cm above soil specimens. In addition, a 150 Watts halogen bulb was used as a light source.

2.4. Spectral preprocessing and analysis

The spectral conversions and preprocessings were done to minimize or omit the disturbing effects and improve the spectra quality. For this purpose, spectral averaging, smoothing and derivations (1st & 2nd) were performed after reviewing the collected spectra. Accordingly, the raw spectra (Fig. 3A) were averaged per 10 nm spectral range (Fig. 3B) and the independent parameters reached 216 spectral data-points. The transformations such as Savitzky-Golay (SGF) smoothing (Fig. 3C), first and
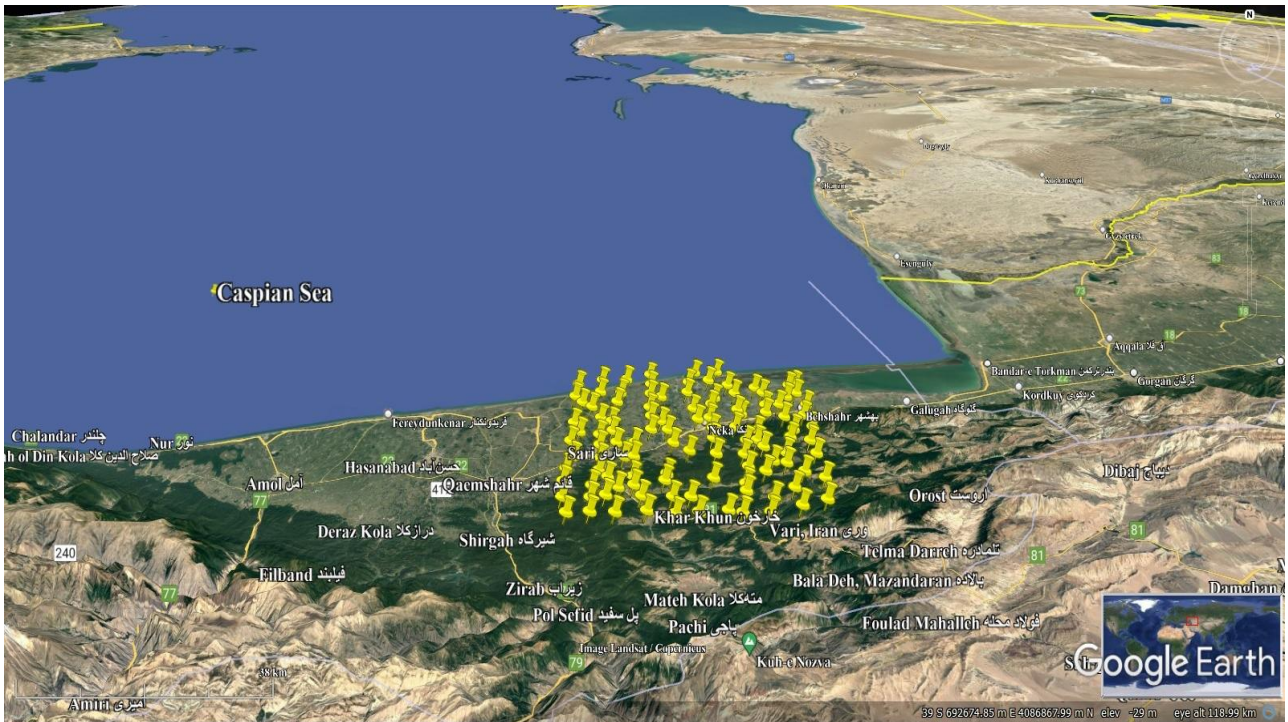
Fig. 1. Location of the sampled points in the eastern parts of Mazandaran Province, Iran.
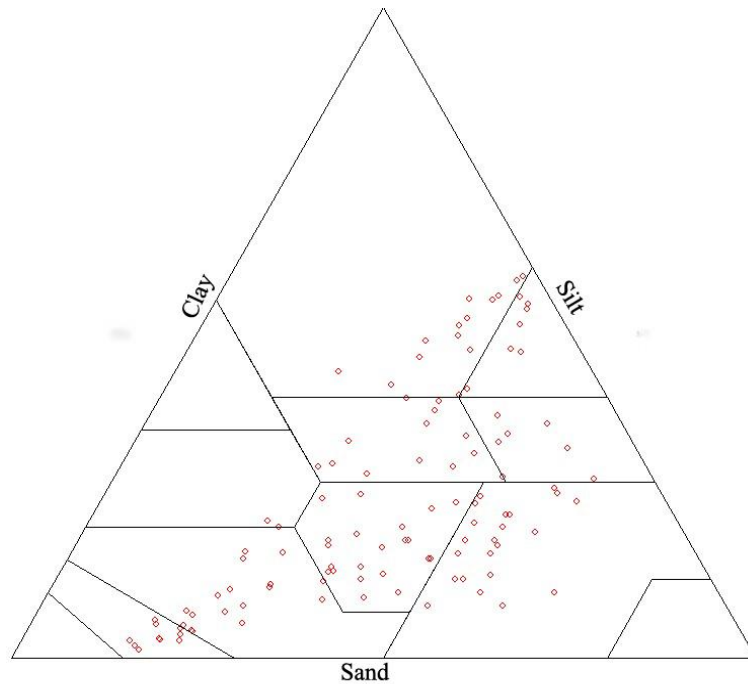

Fig. 2. Soil textural classes of the sampled points in eastern parts of Mazandaran Province, Iran.

second derivatives (1st & 2nd -D) and mean-centering conversion were also processed on the raw reflected spectra (Fig. 3D-F). The full cross validation (FCV) algorithm was also done to choose the best spectral transformation and preprocessings (Casa *et al.*, 2013).
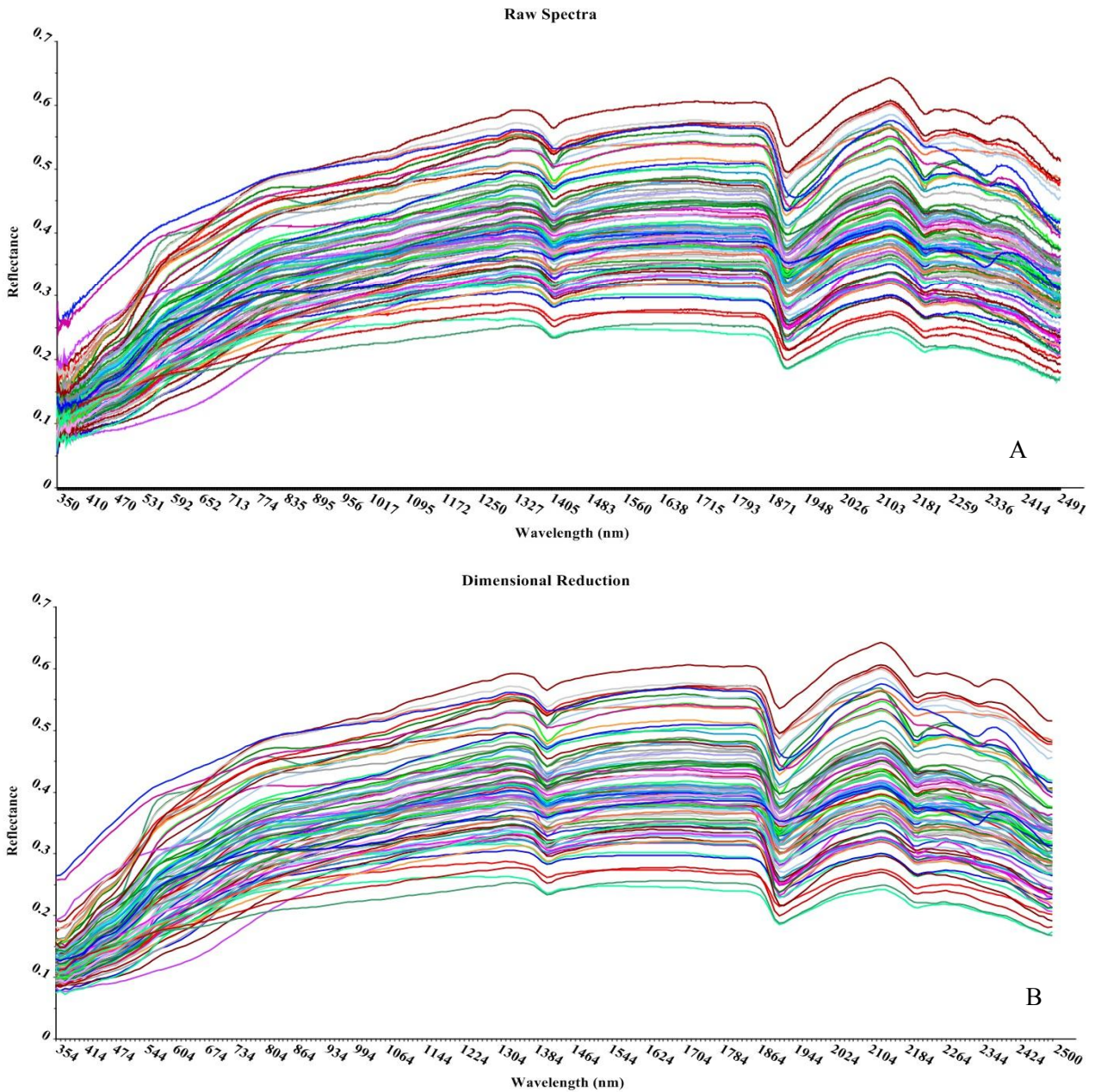
Raw Spectra

Dimensional Reduction

Fig. 3. Spectral conversions and pre-processing, A) raw spectra, B) reduced spectra, C) smoothed with SG filter, D) transformed based on 1st-derivative algorithm and E) transformed based on 2nd-derivative algorithm.

2.5. Spectral-statistical approach

There are different chemometric approaches to extract information from soil reflected spectra. All of these chemometric approaches aim to connect the reflected spectra to the soil properties of interest (Hong *et al.*, 2019). The Partial Least Squares Regression (PLSR) algorithm which was adopted and utilized in this research, is one of the most and best of them which is widely utilized (Zhao *et al.*, 2020). This algorithm with a vigorous approach due to availing the benefits of MLR

and PCA arithmetic procedures together, yielding uniform and precise results for a wide range of soils.

3. Results and Discussion
3.1. Statistical properties of soil textural components

According to the descriptive statistics for textural components of sampled points, the sand fraction showed the means: 37.3%, range: 80.7% and CV about 60.2 %. For clay fraction, they were: 23.6%, 57.3% and 67.2%. Also, for silt contents they were: 39.1, 53.3 and 33.4%, respectively (Table 1)**.**
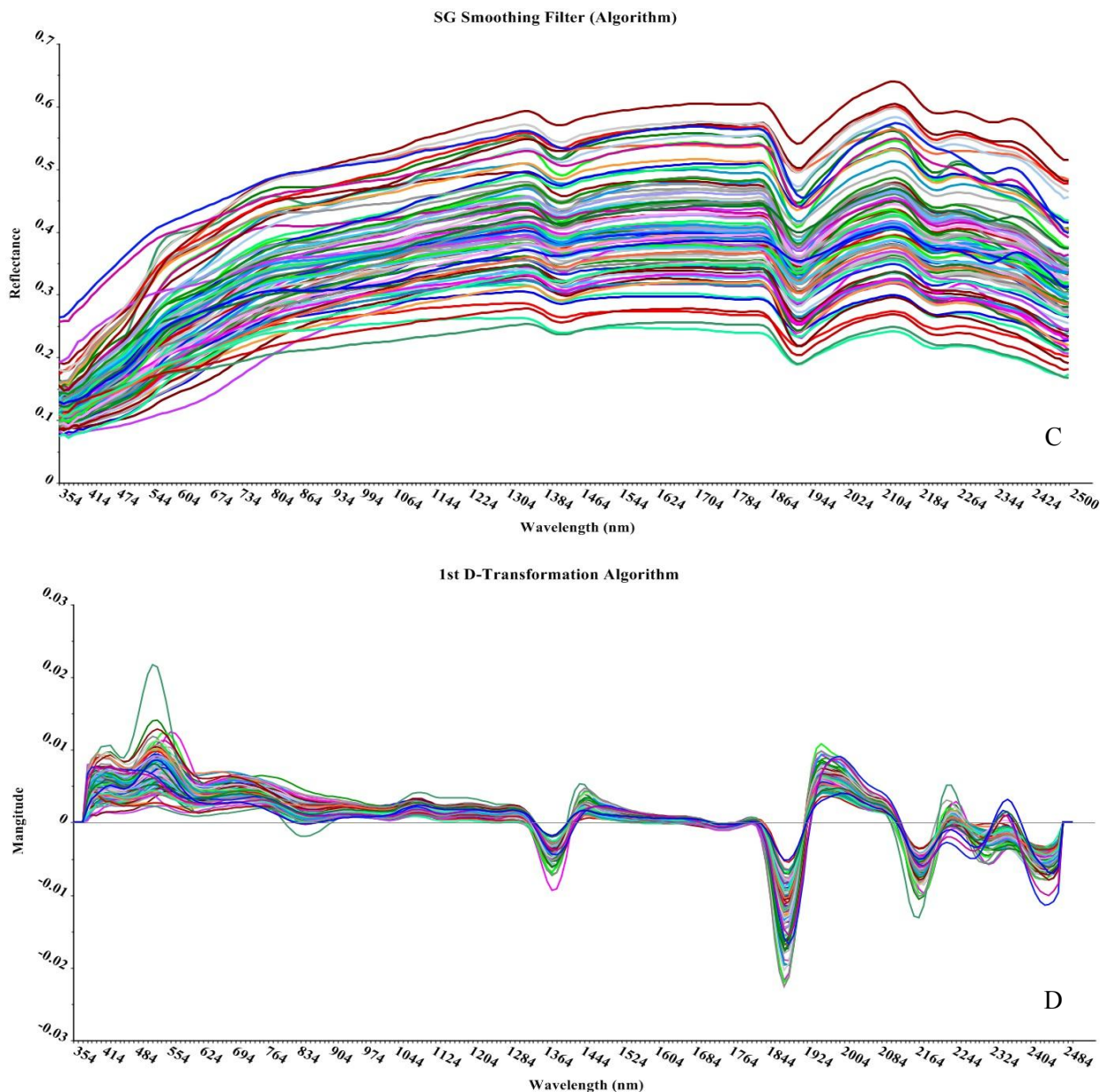
SG Smoothing Filter (Algorithm)

1st D-Transformation Algorithm

Fig. 3. (continued)

3.2. Modeling process

First, the total samples were haphazardly divided into two groups: 91 for modeling process and 22 for final evaluation and accuracy assessment. In addition, the similarity assays such as *KS*, *Student's t* and *Levene's tests* were performed between two groups which respectively showed the similarity of normality, means and variances in both groups. The full leave one out cross validation (FLOOCV) calibration approach was selected as the best technique to get the optimum number of latent factors/latent vectors (LF/LV). On the other hand, it can manage high CV's of parameters and minimize the multi-

collinearity and autocorrelation errors between predictors and responses (Guo *et al.*, 2019). As an important stage in the modeling operation, the scoring process was done to concentrate the variances and reduce the similarities between predictors and responses. Therefore, the first 2 LFs centralized 98% of spectral data and 74% of soil data individually (Fig. 4A). Accordingly, the process of PCA was based on the 7 final latent factors (LF) as a default. FLOOCV technique found the best PCs/LFs for each soil component. This advanced analytical approach is used to avoid the under- or over-prediction of dependent variables (Lu *et al.*, 2013). Based on the regression coefficient (R^2_{CV}), root mean square of error ($RMSE_{CV}$)
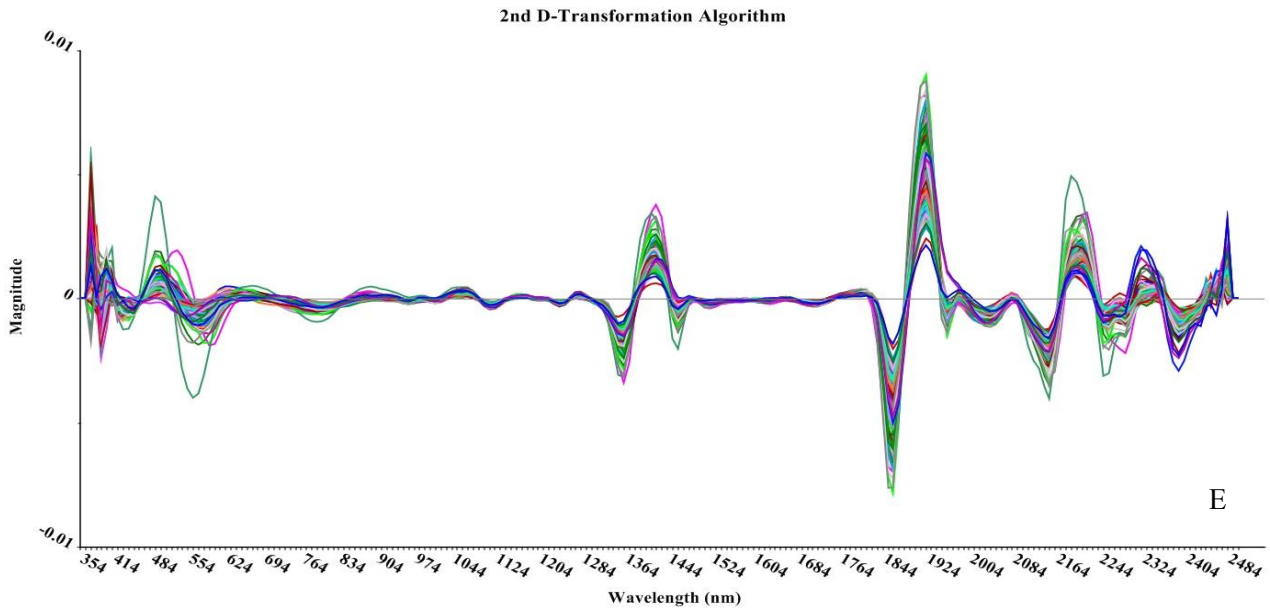
2nd D-Transformation Algorithm

Fig. 3. (continued)

Table 1. The descriptive statistics of soil textural components in the study area.

VOI	Min	Max	Skewness	Kurtosis	Mean	Median	SD	Range	CV%
Sand	2	82.7	0.45	-0.83	37.26	32	22.44	80.7	60.2
Clay	1.2	58.5	0.65	-0.64	23.6	19.2	15.87	57.30	67.2
Silt	14.7	68	0.053	-0.85	39.13	39	13.07	53.30	33.4

and correlation coefficient (R_{cv}), the best LFs/PCs for textural components were determined as follows: 6 LFs for sand component, 7 LFs for clay component and 6 LFs for silt component (Fig. 4A-K). The *IFt*, *Hotelling T^2* and *Adjusted Leverage* (*ALT*) *tests* also showed the participation of more than 92% of spectral and soil samples together in building the final model (Fig. 4E). The leverage was automatically set and then the heterogeneity of spectral data was investigated (Fig. 4-R,S). The effective wavelengths and spectral domains were characterized via assays consisting of *beta & spectral weight analyses* and *Marten's uncertainty tests* (Fig. 4L-Q). Therefore, the best effective wavebands contributing in estimation of soil texture components were well-defined. In the eastern parts of Mazandaran soils, the spectral ranges of visible, NIR and SWIR were recognized to be influential in studying soil texture (Fig. 4L-Q). The next step was dedicated to modeling the final calibrated relationship between constituents (LFs) and spectral data (Fig. 5A-C). At the same time, checking the residuals related to the soil and spectra data via *IFt* (influence test) has proved the effectiveness of the model. Final predictive model for each components was calibrated using PLS algorithm along with the FLOOCV technique with specified indices as follows for sand

fraction: R_c= 0.94, R^2_c= 0.89, $RMSE_c$ = 7.42 and SE_c = 7.46; for clay fraction: R_c= 0.90, R^2_c= 0.82, $RMSE_c$ = 6.88 and SE_c = 6.92; and for silt component: R_c= 0.62, R^2_c= 0.39, $RMSE_c$ = 10.21 and SE_c = 10.27. As stated earlier, the finalized calibrated models for sand and silt were based on 6 LFs and for clay, the model was based on 7 LFs. Also, the specifications of each model are presented in the box of Fig. 5A-C. The accuracy and quality of the calibrated models were computed by taking advantage of the indicants of model accuracy, RPD and RPIQ (Bellon-Maurel *et al.*, 2010; Chang and Laird, 2002). Therefore, the quality and efficiency of calibrated model were as the following: for sand fraction, RPD_c = 3.08, $RPIQ_c$ = 4.81, for clay fraction, RPD_c = 2.36, $RPIQ_c$ = 3.46 and for silt fraction, RPD_c = 1.29 and $RPIQ_c$ = 2, respectively. Also, the maximum correlations between the textural constituents and the spectral domains were calculated applying the multi-component approach (Fig. 4L-Q). Correspondingly, they are as the following: for sand: visible-610 nm (0.75), NIR-970 nm (0.81) and SWIR-2200 nm (0.92), for clay: visible-550 nm (-0.63), NIR-950 nm (-0.80) and SWIR-2000-2400 nm (088-0.89). As for silt: visible-470 nm (-0.39), NIR-1040 nm (-0.50) and SWIR-1910-2220 nm (-0.51 to -0.53) (Fig. 4L-Q). Consequently, the selected spectral
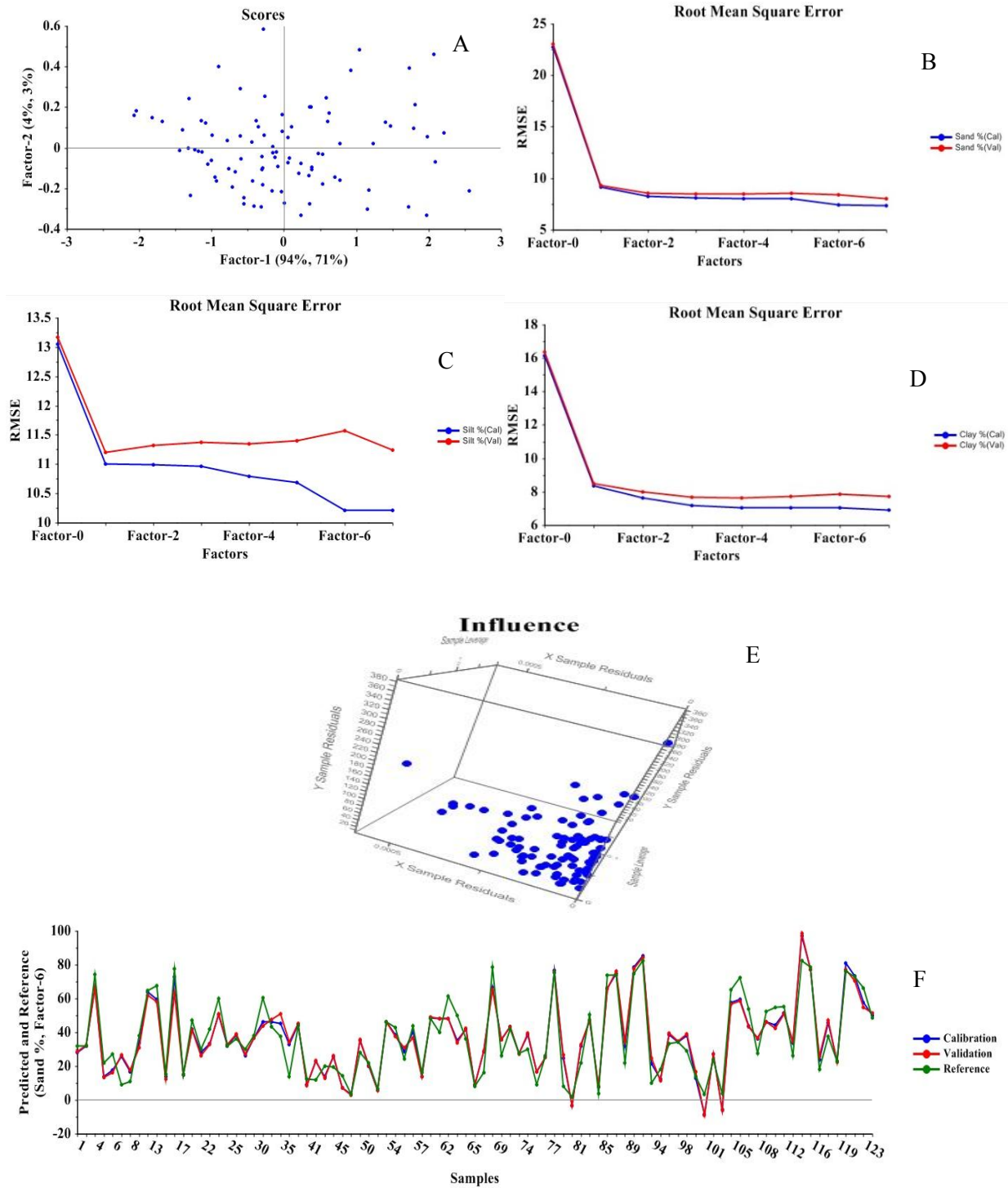
Fig. 4. Outputs of PLSR algorithm in brief, A) analysis of principle components (scoring process) based on soil components and spectral data; B,C,D) FLOOCV-auto-selection of LFs/LVs based on RMSE analyses for sand, clay and silt fraction, respectively; E) influence test on residuals and leverage to prove the effectiveness of predictors and response; F,G,H) predicted and reference amounts of sand, clay and silt, respectively, on the basis of choice LFs in calibration-FLOOCV approach; I,J,K) predicted components vs checking out the reference amounts for sand, clay and silt, correspondingly; L,M,N) results of Marten's uncertainty test, weighted beta coefficients and analysis of regression coefficients (Single-Beta) to detect and define the most influential spectral ranges, wavebands and zero-effect wavelengths for sand, clay and silt; O,P,Q) characterization of effective wavelengths according to X-loading weight analysis for sand, clay and silt, respectively; R) residual sample calibration variance for response data; S) the final leverages according to LFs and samples in modeling process.
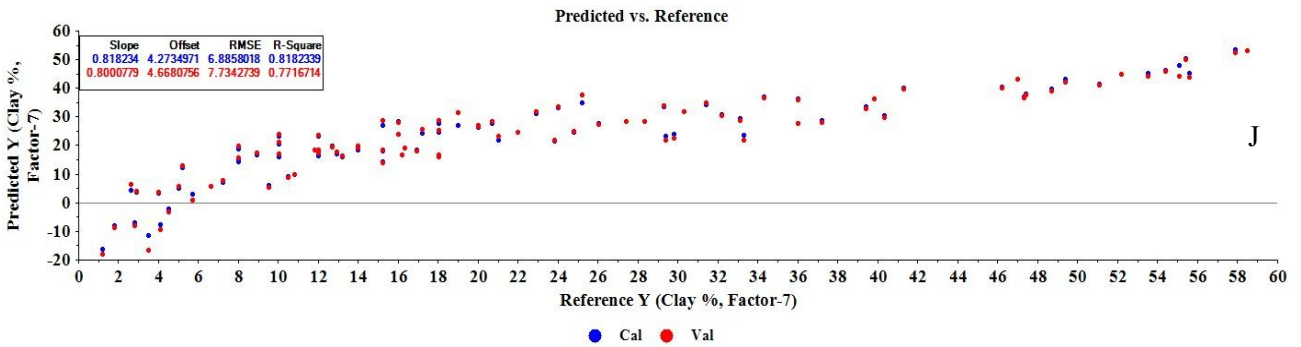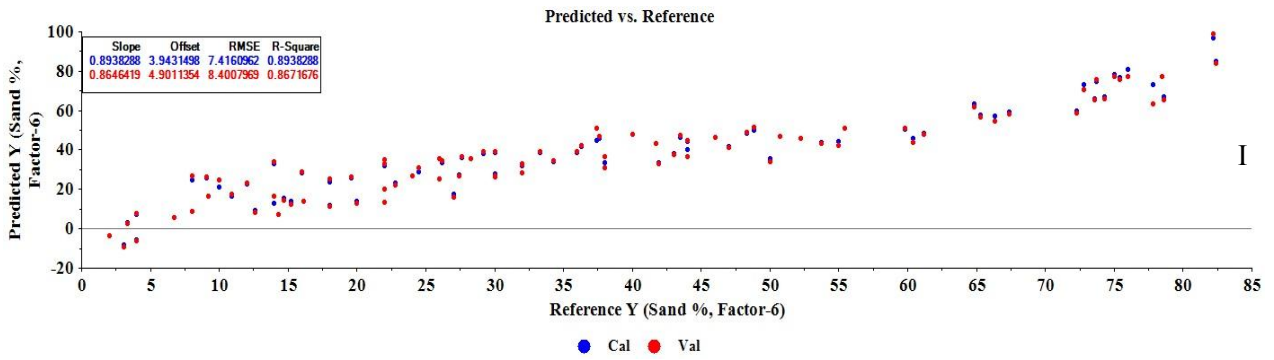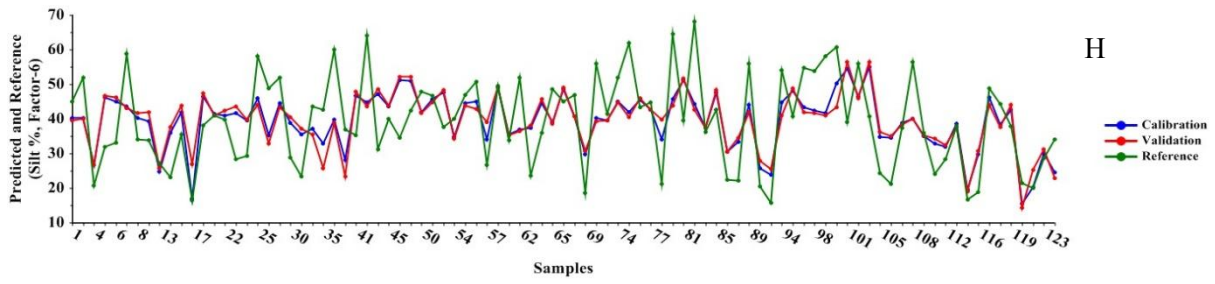
G

H

I

J

K

Fig. 4. (continued)

31

Fig. 4. (continued)

Q

X-loading Weights

R

Leverage

S

Residual Sample Calibration Variance
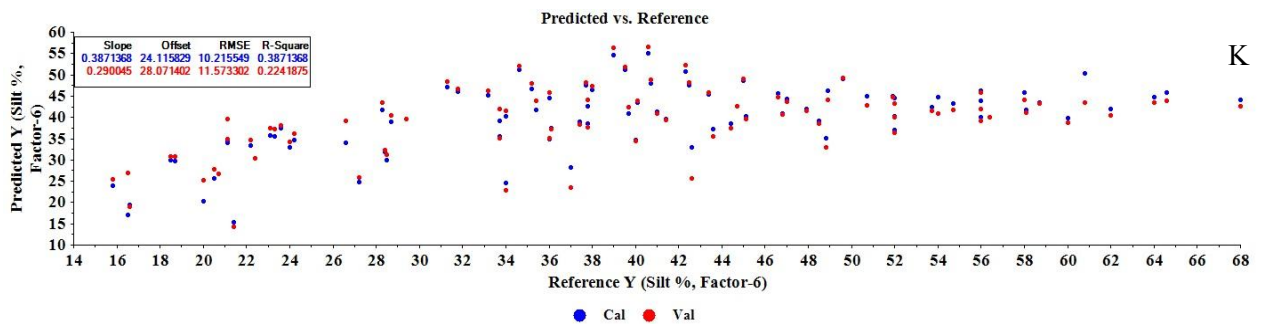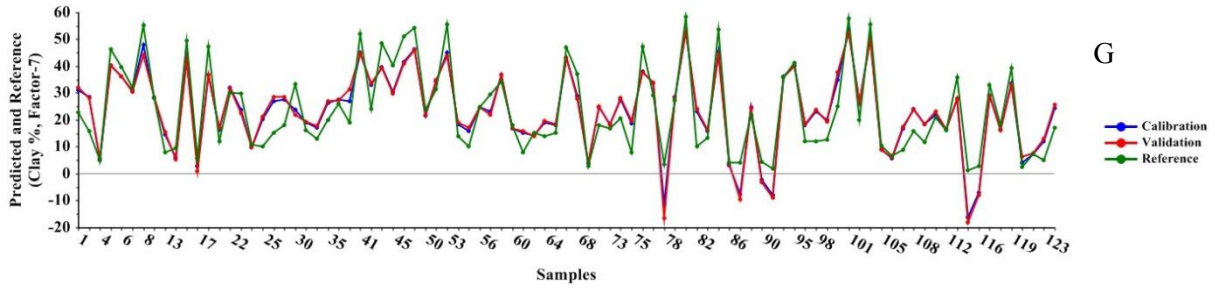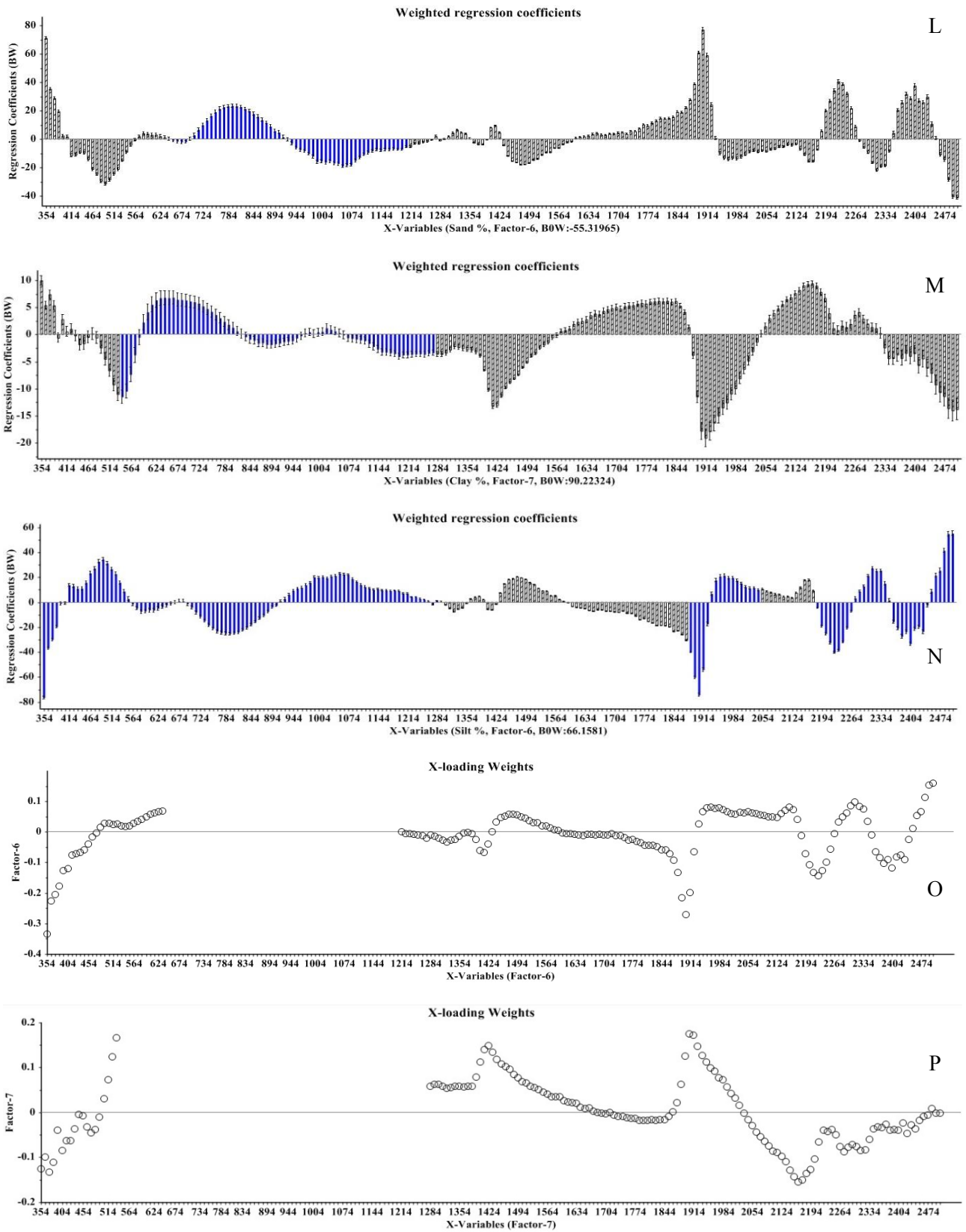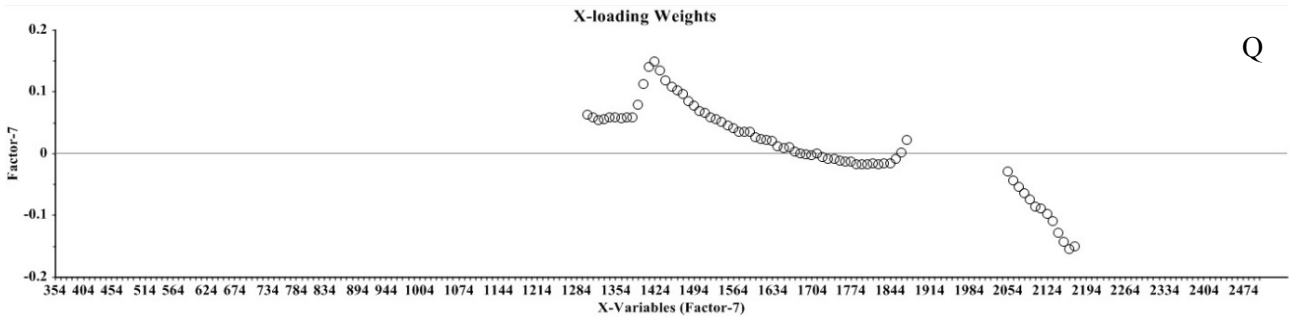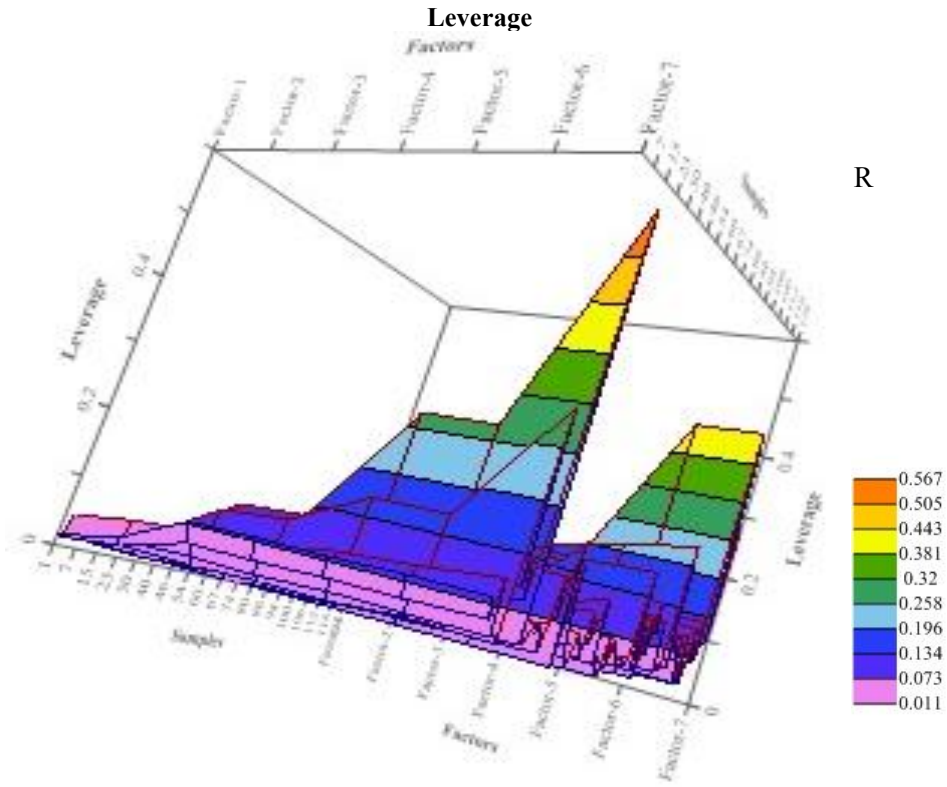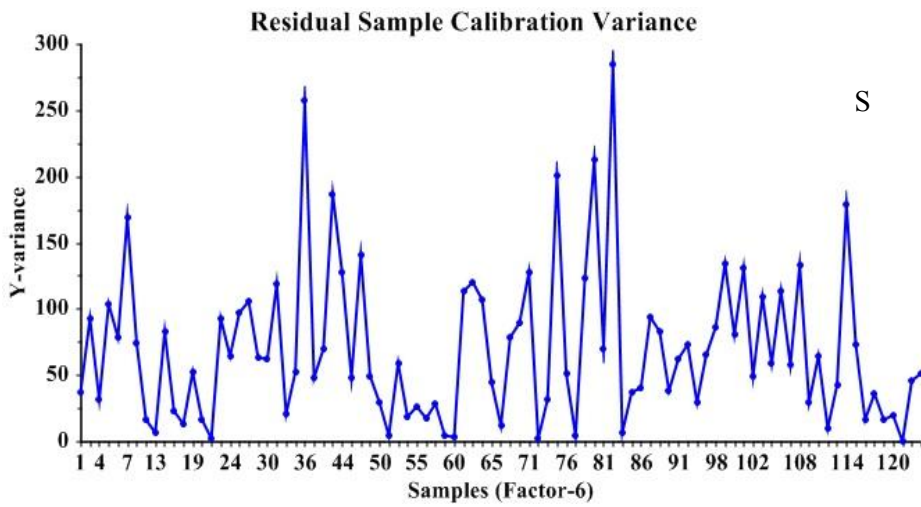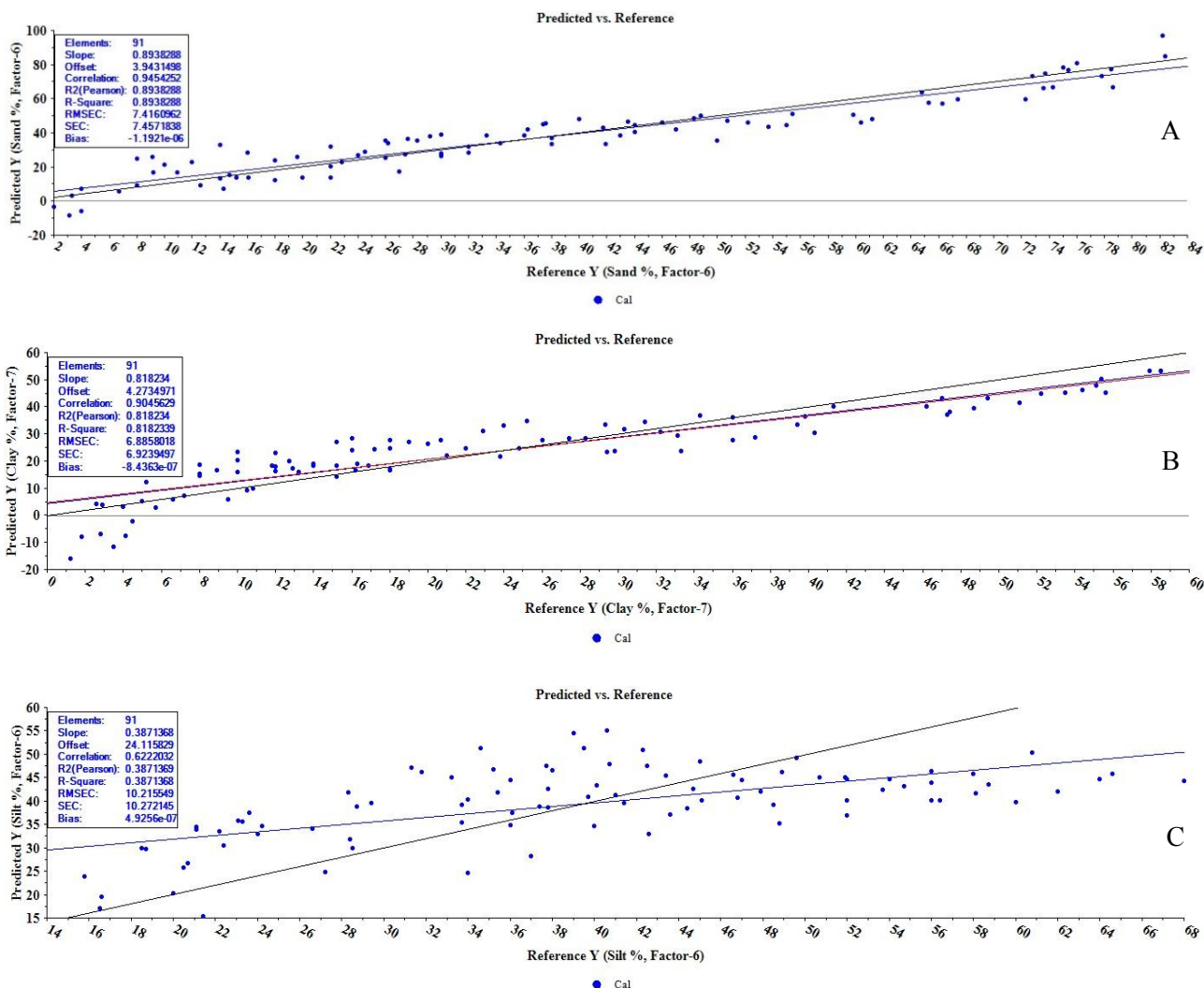
Fig. 4. (continued)

Fig. 5. A, B, C) Outputs of fully described finalized model with the relevant parameters after checking all items, according to the specific LF/LV for sand, clay and silt fractions, respectively.

domains and wavebands with highest correlations show the best effects of reflected spectra in the modeling of textural components in the soils of the studied region. Unquestionably, in this research, the vibrational reflected spectra of the soil surface contain the valuable information about the soil constituents of Mazandaran province, Iran.

3.3. Assessment of model accuracy

The validation and verification steps of the calibrated models were fulfilled using 22 independent soil samples. For this, the finalized calibrated models for each textural component were utilized to predict just the same case in the validation group samples. Accordingly, the built models for sand, clay and silt fractions based on 6, 7 and 6 LFs, respectively, were prepared for validation process. The predicted soil components using this step were compared to the reference values of the independent

samples (Fig. 6A-C). Then, the accuracy and precision of each of the models were appraised (Fig. 7A-D). Scientifically, the parsimonious models based on the fewer LFs/LVs/PCs are preferred (Figs. 6 and 7). Hence, the validation process set the models free to choose the best and less number of LFs for each textural component (Danesh and Bahrami, 2022).

Figures 6 and 7 represent the predicted vs measured values for soil texture fractions using the finalized model for independent samples. Therefore, the sand model was assessed with: correlation coefficient (Rp) = 0.88, regression coefficient (R^2p) = 077, RMSEp = 10.23 and SEp = 10.09. The clay model also was validated with: Rp = 0.83, R^2p = 0.69, RMSEp = 7.99 and SEp = 8.26. Also the silt model was verified as: Rp = 0.49, R^2p = 0.24, RMSEp = 11.37 and SEp = 12.20. In addition, the prediction process with deviations demonstrated in Fig. 7A-D diagrammatically. Figure 7D shows the leverage
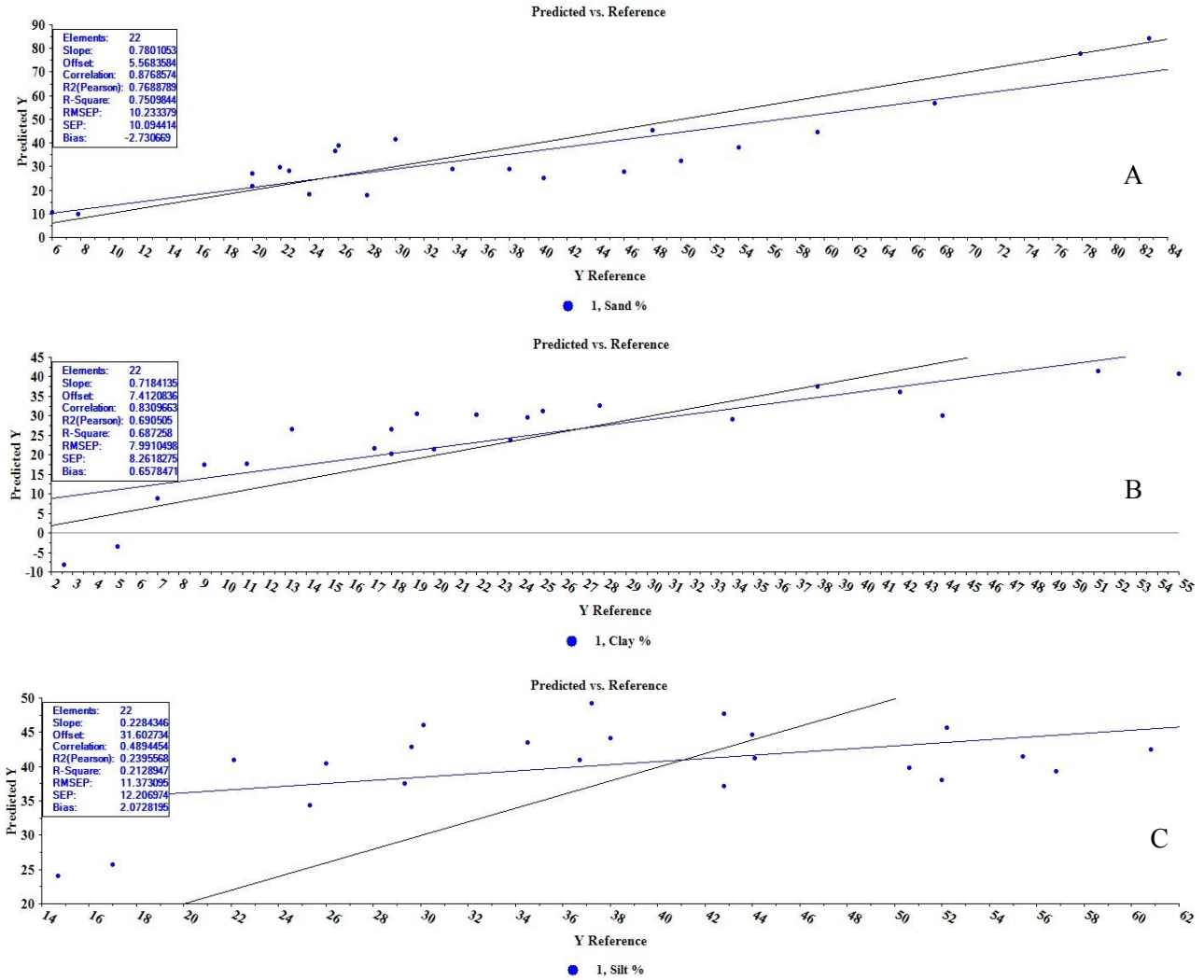
Fig. 6. The final verification and accuracy assessment of models in accordance with the independent samples for A) sand, B) clay and C) silt fractions. (All modeled relationships are based on the FLOOCV-PLS-algorithm).

values based on the principal components involved in the model assessment. As an estimation, according to the prediction process of soil components, their deviations and the involved leverages (Figs. 6 and 7), it can be concluded that the modeling processes were definitely acceptable and well-structured. Computationally, the efficiency and quality of the models were evaluated using two model robustness factor named RPDp and RPIQp. Therefore, the models were qualified for sand with specifications including: RPDp = 2.05, RPIQp = 2.79; for clay: RPDp = 1.83, RPIQp = 2.78, and finally for silt: RPDp = 1.15 and RPIQp = 1.98. The prediction ability for soil properties can be divided into three categories based on the RPD/RPIQ values. Generally, if the indices of the model are (calibrating/validating step) > 2.0, the model is Grade A, indicating a very good and precise prediction of soil characteristics. If it is between 1.4 and 2.0, the model is classified as Grade B, suggesting that

the model ability of prediction and its efficiency to be acceptable to good. If it is < 1.4, the model is Grade C, indicating the insufficiency and inappropriateness of the model power to predict the properties (Chang and Laird, 2002). According to the results in the model building and evaluation steps, the sand model in the calibration step with calculated RPDc = 3.08 and RPIQc = 4.81 is very good and robust to predict this component in Mazandaran soils. That was also proved in the evaluation process using independent samples with RPDp = 2.05 and RPIQp = 2.79. As compared to the results provided by Danesh and Bahrami (2022), and Bahrami *et al.* (2022), the current sand model has performed much better and more powerful. The clay model in the building stage with RPDc = 2.36 and RPIQc = 3.46 showed similar vigorous ability to assess this fraction. This was confirmed in the evaluation stage by RPDp = 1.83 and RPIQp = 2.78. Also, according to the model parameters and quality
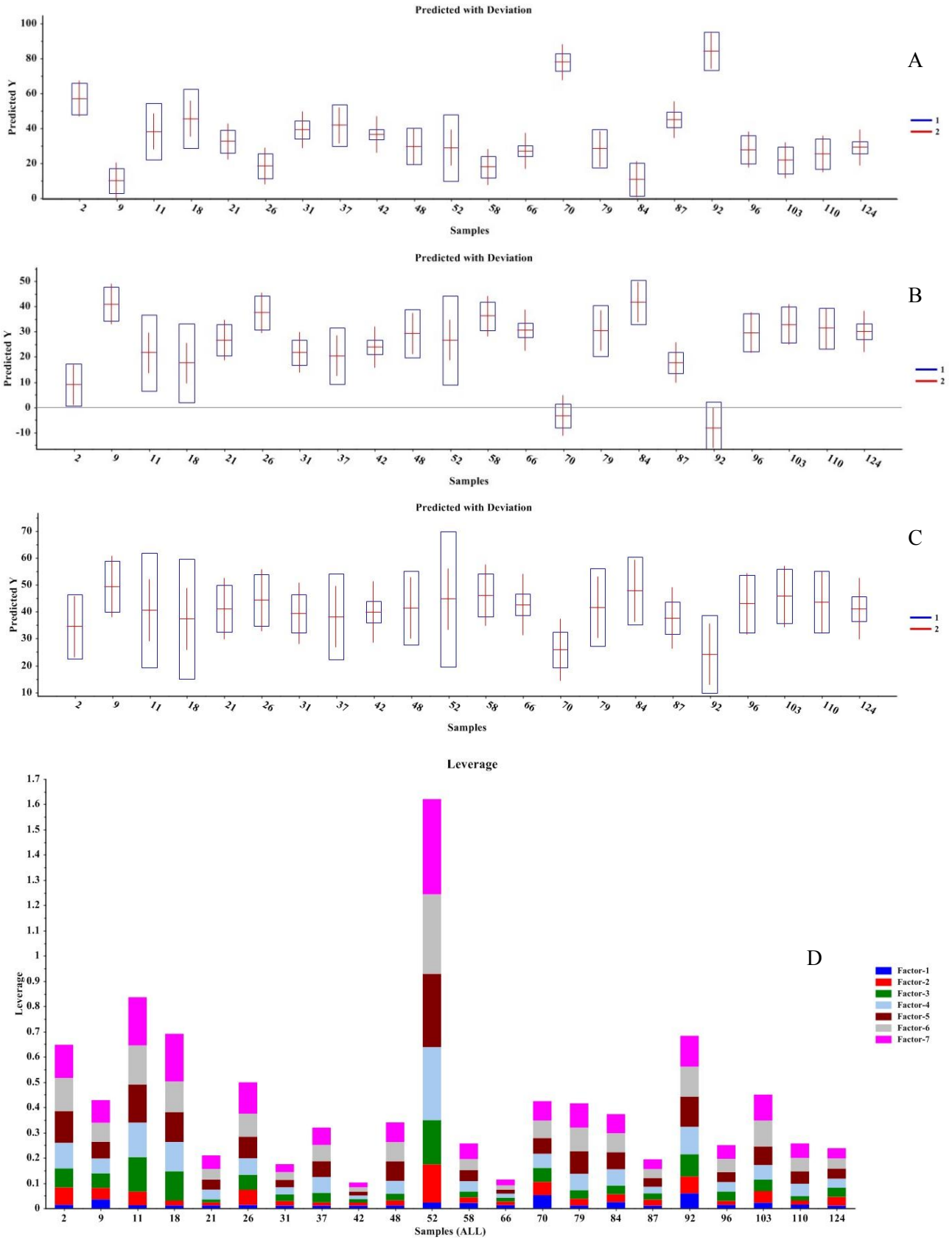
Fig. 7. Predicted values with deviation for each sample in the validation step for: A) sand, B) clay and C) silt components; D) examining of leverage values for each LF in the validation samples.

indicators, the current clay model is more accurate, competent and reliable comparing to the research done by Danesh *et al.* (2016). But for silt fraction, the dedicated model performed relatively weaker in both steps like the calibration stage with RPDc = 1.29 and RPIQc = 2. Similarly, for the validation step with RPDp = 1.15 and RPIQp = 1.98, they were somewhat weaker but showed the acceptable to moderately weak prediction of this textural constituent. In the same way, the results for silt constituent were partly consistent with the study done by Danesh *et al.* (2022). In addition, Peng *et al.* (2020), studied soil texture fractions in China using spectroscopy and PLS enhanced algorithm. They were able to estimate sand fraction with $R^2 = 0.77$, clay with $R^2 = 0.65$ and silt with $R^2 = 0.71$. Compared to their results, the present study was more effective and accurate in predicting sand and clay fractions, but not for silt fraction. Also Zhao *et al.* (2020) as well as Xu *et al.* (2018 ab) investigated clay particles with the similar model quality. The model built by Xu *et al.* (2018) was more accurate for silt constituents because of its appropriate CV% and variability range. Zeng *et al.* (2017) performed an investigation to predict the texture using vibrational technology and ten-fold cross-validated PLSR modelling approach. Their model parameters were as follows for clay: $R^2adj = 0.60$, RMSEcv = 3.18 and RPD = 1.57 which was relatively weaker than the current clay predicting model. For silt component: $R^2adj = 0.78$, RMSEcv = 10.20 and RPD = 2.11 that was more powerful and precise than the present silt model. Also for sand fraction, they reached $R^2adj = 0.78$, RMSEcv = 12.19 and RPD = 2.06 that was somewhat weaker than the results of our research. The reasons for the silt component model being weaker than other fractions are the low values of coefficient of variation (CV %) for silt besides the low variability range plus the kurtosis value of the VOI.

4. Conclusions

Comparing to traditional methods, the present research showed the applicability of spectroscopic technology to predict the components of soil texture more quick, timely, inexpensive, repeatable and nondestructive. This applied technology utilized spectral features in the whole reflected spectra. Definitely, the advanced approach composed of chemometric methods and VNIR technology made this study possible. Also, main spectral preprocessing and FLOOCV algorithm resulted in the precise and accurate models for each soil fraction. Also, using the quality and accuracy indicators of modeling processes, it was shown that the model efficiency and ability have been higher than some similar studies. Finally, it can be concluded that the spectral model for sand and clay components has performed excellently. But for the silt fraction, the model function was somewhat weaker compared to some relevant studies. This demands more samples from different geographical areas with more variation ranges to be taken. In addition, the influential spectral domains in prediction of soil texture were determined as visible, NIR and SWIR ranges. Applying these spectral ranges and wavelengths, gives the capability to study the soil textural characteristics at large scales using remotely sensed data.

References

Bahrami, A., Danesh, M., & Bahrami, M. (2022). Studying sand component of soil texture using the spectroscopic method. *Infrared Physics & Technology, 122*, 104056.

Bellon-Maurel, V., Fernandez-Ahumada, E., Palagos, B., Roger, J. M., & McBratney, A. (2010). Critical review of chemometric indicators commonly used for assessing the quality of the prediction of soil attributes by NIR spectroscopy. *TrAC Trends in Analytical Chemistry, 29 (9)*, 1073–1081.

Camargo, O. A., Moniz, A. C., Jorge, J. A., & Valadares, J. M. (2009). Methods of Chemical, Mineralogical and Physical Analysis of Soils Used in the Pedology Section (Technical Bulletin No. 106), Instituto Agronômico (IAC), Campinas.

Casa, R., Castaldi, F., Pascucci, S., Palombo, A., & Pignatti, S. (2013). A comparison of sensor resolution and calibration strategies for soil texture estimation from hyperspectral remote sensing. *Geoderma, 197*, 17–26.

Chang, C. W., & Laird, D. A. (2002). Near-infrared reflectance spectroscopy analysis of soil C and N. *Soil Science, 167*: 110–116.

Danesh, M., Bahrami, H. A., Darvishzadeh, R., & Noroozi, A. A. (2016). Investigating clay contents using laboratory diffuse reflectance spectroscopy. *Iranian Journal of Remote Sensing & GIS, 8*(1), 71-94. (In Persian).

Danesh, M., Bahmanyar, M. A., & Emadi, S. M. (2022). Reflectance study of soil silt using proximal sensing in Northern Iran. *Journal of Civil Engineering and Environmental Sciences, 8(1),* 048-056.

Danesh, M., & Bahrami, H. A. (2022). Modeling of Soil Sand Particles Using Spectroscopy Technology, *Communications in Soil Science and Plant Analysis, 53,* 2216-2228.

Emadi, M., Taghizadeh-Mehrjardi, R., Cherati, A., Danesh, M., Mosavi, A., & Scholten, T. (2020).

Predicting and mapping of soil organic carbon using machine learning algorithms in Northern Iran. *Remote Sensing*, *12*(14), 2234.

Guo, L., Zhang, H., Shi, T., Chen, Y., Jiang, Q., & Linderman, M. (2019). Prediction of soil organic carbon stock by laboratory spectral data and airborne hyperspectral images. *Geoderma*, *337*, 32-41.

Hong, Y., Chen, S., Liu, Y., Zhang, Y., Yu, L., Chen, Y., & Liu, Y. (2019). Combination of fractional order derivative and memory-based learning algorithm to improve the estimation accuracy of soil organic matter by visible and near-infrared spectroscopy. *Catena*, *174*, 104–116.

Ji, W. J., Li, S., Chen, S. C., Shi, Z., Viscarra Rossel, R. A., & Mouazen, A. M. (2016). Prediction of soil attributes using the Chinese soil spectral library and standardized spectra recorded at field conditions. *Soil Tillage & Research*, *155*, 492–500.

Ji, W. J., Shi, Z., Huang, J. Y., & Li, S. (2014). In situ measurement of some soil properties in paddy soil using visible and near-infrared spectroscopy. *PLoS ONE, 9(8),* e105708.

Lu, P., Wang, L., Niu, Z., Li, L., & Zhang, W., (2013). Prediction of soil properties using laboratory VIS–NIR spectroscopy and Hyperion imagery, *Journal of Geochemical Exploration*, *132*, 26–33.

Mura, S., Cappai, C., Greppi, G. F., Barzaghi, S., Stellari, A., & Cattaneo, T. M. P. (2019). Vibrational spectroscopy and Aquaphotomics holistic approach to determine chemical compounds related to sustainability in soil profiles. *Computers and Electronics in Agriculture*, *159*, 92–96.

Ostovari, Y., Ghorbani-Dashtaki, S., Bahrami, H. A., Abbasi, M., Dematte, J. A. M., Arthur, E., & Panagos, P. (2018). Towards prediction of soil erodibility, SOM and $CaCO_3$ using laboratory Vis-NIR spectra: A case study in a semi-arid region of Iran. *Geoderma*, *314*, 102-112.

Padarian, J., Minasny, B., & McBratney, A. B. (2019). Using deep learning to predict soil properties from regional spectral data. *Geoderma Regional*, *16*, e00198.

Peng, L., Cheng, H., Wang, L. J., & Zhu, D. (2020). Comparisons the prediction results of soil properties based on fuzzy c-means clustering and expert knowledge from laboratory Vis-NIR spectroscopy data. *Canadian Journal of Soil Science*, *101*(1), 33-44.

Pudełko, A., & Chodak, M. (2020). Estimation of total nitrogen and organic carbon contents in mine soils with NIR reflectance spectroscopy and various chemometric methods. *Geoderma*, *368,* 114306.

Qi, F., Zhang, R., Liu, X., Niu, Y., Zhang, H., Li, H., Li, J., Wang, B., & Zhang, G. (2018). Soil particle size distribution characteristics of different land-use types in the Funiu mountainous region. *Soil & Tillage Research*, *184*, 45-51.

Tumsavas, Z., Tekin, Y., Ulusoy, Y., & Mouazen, A. M. (2018). Prediction and mapping of soil clay and sand contents using visible and near-infrared spectroscopy. *Biosystems Engineering. 177,* 90-100.

Viscarra Rossel, R. A., & Webster, R. (2012). Predicting soil properties from the Australian soil visible-near infrared spectroscopic database. *European Journal of Soil Science*, *63*, 848–860.

Xia, F., Peng, J., Wang, Q. L., Zhou, L. Q., & Shi, Z. (2015). Prediction of heavy metal content in soil of cultivated land: hyperspectral technology at provincial scale. *Journal of Infrared Millim. Waves*, *34*, 593–605.

Xu, D., Ma, W., Chen, S., Jiang, Q., He, K., & Shi, Z. (2018a). Assessment of important soil properties related to Chinese Soil Taxonomy based on vis–NIR reflectance spectroscopy. *Computers and Electronics in Agriculture*, *144*, 1-8.

Xu, S., Zhao, Y., Wang, M., & Shi, X. (2018b). Comparison of multivariate methods for estimating selected soil properties from intact soil cores of paddy fields by Vis–NIR spectroscopy. *Geoderma*, *310*, 29-43.

Zhao, L., Hong, H., Fang, Q., Algeo, T. J., Wang, C., Li, M., & Yin, K. (2020). Potential of VNIR spectroscopy for prediction of clay mineralogy and magnetic properties, and its paleoclimatic application to two contrasting Quaternary soil deposits. *Catena*, *184*, 104239.

Zeng, R., Rossiter, D. G., Yang, F., Li, D. C., Zhao, Y. G., & Zhang, G. L. (2017). How accurately can soil classes be allocated based on spectrally predicted physico-chemical properties? *Geoderma*, *303*, 78–84.